

ORIGINAL RESEARCH ARTICLE

The Assessment of the Adsorption Capacity of Sorghum Husk for Phenol Remediation

Obianuju Leticia Nwanji^{1*} and Chinenye Goodness Iweatu¹¹Department of Chemistry, Alex Ekwueme Federal University Ndufu Alike, Ebonyi State, Nigeria

ABSTRACT

Phenol is used in many industries; hence, effluents from these industries should be treated properly in order to avert environmental pollution. One of such treatment methods is adsorption, where agricultural waste such as sorghum husk can be used as adsorbents. The main purpose for carrying out this research was to ascertain the efficacy of sorghum husk (SH) as an adsorbent for remediating phenol from water. The SH was characterized with the use of pH at zero point charge (pH_{Zpc}), Fourier transforms infrared (FTIR) spectroscopy and Sear's surface area analysis. The effects of some factors that affect adsorption were examined in batches. The data emanating from the adsorption batch experiments were analysed with isotherm and kinetic models. Thermodynamic parameters that examine the adsorption process's heat, randomness, and spontaneity were assessed. The pH_{Zpc} of the SH adsorbent was 6.2, and the FTIR spectra displayed typical peaks representing functional groups that are essential for adsorption. The Sear's surface area of SH was 77.40 m² g⁻¹. The most favourable conditions for the highest adsorption were achieved at the pH of 10, adsorbent dose of 5 mg, phenol initial concentration of 70 mg L⁻¹, and temperature of 55 °C. The adsorption equilibrium was described well by the Freundlich model, while the description of the kinetics was done better by the pseudo-second-order model. The thermodynamic assessment of the adsorption process suggested that it was endothermic, random, and spontaneous. The proposed mechanism of adsorption was physical adsorption. This research showed that sorghum husk is an efficient adsorbent for the remediation of phenol.

ARTICLE HISTORY

Received March 26, 2025

Accepted May 20, 2025

Published June 09, 2025

KEYWORDS

Adsorption, isotherm, kinetics, phenol, sorghum husk, thermodynamics



© The Author(s). This is an Open Access article distributed under the terms of the Creative Commons Attribution 4.0 License [creativecommons.org](https://creativecommons.org/licenses/by-nc/4.0/)

INTRODUCTION

According to WHO, almost 80% of effluents are not properly treated before discharge, posing a high risk of health hazard and diseases to the communities where these effluents are discharged (Tshemese et al., 2021). Wastewater from industries, homes, and agricultural activities contains high levels of pollutants that should be treated before discharge to avoid environmental pollution (Dehmani et al., 2023). Many industries use phenol as a starting material for production; hence, phenol is present in the industrial effluents from industries such as refineries, coal plants, petrochemical industries, resin manufacturing industries, pharmaceutical industries, and so on (Guo et al., 2019; Lv et al., 2020). Phenol is toxic, and because it is easily absorbed in the body, it can cause damage to the skin, respiratory tract, mucous membrane, liver, kidney, and immune system (Lv et al., 2020; Sabbar, 2019; Wang et al., 2020).

Many methods, such as membrane filtration, coagulation, photocatalytic degradation, adsorption, ion exchange precipitation, and solvent extraction, have been utilised for wastewater remediation (Dehmani et al., 2023; Guo et

al., 2019). It has been said that adsorption is a cheap, versatile, and efficacious method utilised for the uptake of many pollutants, including phenol (Issabayeva et al., 2018; Sellaoui et al., 2019). Adsorptive materials such as activated carbon and biochar have excellent performance, but they are expensive to produce relative to cheaper adsorbents that are obtained from waste (Xu et al., 2022). Agricultural wastes have been used widely for adsorption because they cost little or nothing, are easy to process, and are readily available (Nnaji et al., 2023). Agricultural waste from cereal such as rice, wheat, sorghum, millet and barley has been effective for adsorption (Shaikhiev, 2024).

Sorghum husk is one of the agricultural wastes obtained from sorghum after the removal of its grains; other wastes from the crop are bran and straw. Nigeria is one of the major sorghum producers, coming only second after the USA (Shaikhiev, 2024). There is then a need to convert waste generated from using and processing products from sorghum. This will help to reduce the landmass that this waste can occupy and mitigate pollution they would cause. The fact that the waste will be converted to adsorbents

Correspondence: Obianuju Leticia Nwanji. Department of Chemistry, Alex Ekwueme Federal University Ndufu Alike, Ebonyi State, Nigeria. ✉ letobianuju@gmail.com.

How to cite: Nwanji, O. L., & Iweatu, C. G. (2025). The Assessment of the Adsorption Capacity of Sorghum Husk for Phenol Remediation. *UMYU Scientifica*, 4(2), 135 – 141. <https://doi.org/10.56919/usci.2542.016>

and used for wastewater treatment is an added advantage (Tatah et al., 2017; Xu et al., 2022). Although agricultural wastes like rice husk and wheat straw have been explored as adsorbents, sorghum husk use remains underexplored in phenol remediation. This study aims to evaluate its potential and compare it with other established adsorbents, providing a low-cost, environmentally friendly solution for water treatment.

For this research, sorghum husk (SH) adsorbent was prepared, characterised, and utilised for the adsorptive phenol removal from water. The influence of some factors on the adsorptive capability of SH was studied. Adsorption isotherm, kinetic, and thermodynamic analyses were done.

MATERIALS AND METHODS

SH adsorbent and adsorbate preparation

Sorghum was obtained from a market in Abakaliki, Ebonyi State, Nigeria. The grains were soaked in water and de-husked after a few hours. The husk was dried under the sun for 1 week and then put in the oven for further drying at 100 °C for 6 h. It was ground, sieved through 400 µm meshes, and then stored in a well-covered container until its use.

The phenol stock solution was prepared by dissolving 1 g of it in distilled water to make up a 1 L solution. Lower concentrations of phenol were then prepared by serially diluting the stock solution. The absorbance of phenol was recorded at 270 nm using a UV spectrophotometer (ThermoFisher Scientific, USA).

SH adsorbent characterisation

The SH characterisation was achieved by pH at zero point charge (pH_{zpc}) using the salt addition method with a little adjustment. The pH (pH_i) of 50 mL each of 0.1 M KNO₃ solution was adjusted to a pH range of 2 – 12 using either 0.1 M HCl or 0.1 M NaOH. To the individual KNO₃ solution, 0.1 g of SH was added, followed by stirring the resulting solution for 48 h. When stirring was done, the solution was set aside to stand briefly, and the final pH (pH_f) was taken. The difference between pH_i and pH_f was noted and a plot of it against pH_i was done. The intersection point on the x-axis of the graph gave the pH_{zpc} (Nnaji et al., 2023). The SH adsorbent was mixed with KBR pellets for the FTIR analysis, and the spectra were obtained using FTIR spectrometer (Perkin Elmer Spectrum 100, USA). Sear's method was employed to obtain the SH surface area. This was achieved by the dissolution of 30 g of NaCl in 150 mL of distilled water and adding 1.5 g of SH to the solution, followed by shaking the solution for 12 min. The pH of the solution was aligned to 4 using 0.1 M HCl, and it was used for titration against 0.1 M NaOH until its pH was raised to 9. The average titre of the NaOH solution (V) used was observed, and the SH surface area was calculated using equation 1 below (Abate et al., 2020; Sears, 1956).

$$S = 32V - 25 \quad (1)$$

Adsorption experiments

The adsorption experiment was done in batches where SH adsorbent (30 mg) was weighed into 30 ml of 50 mg L⁻¹ phenol solution and was shaken for 1 h at 150 rpm within the following ranges of factors: pH range of 2 to 10 (pH study), 5 to 50 mg (adsorbent dose study), 3 to 70 mg L⁻¹ (initial concentration study), 1 to 180 min (contact time study) and 20 to 55 °C (thermodynamic study). After agitation, centrifugation was done, and the supernatant was analysed for concentration after adsorption using a UV spectrophotometer at 270 nm. The calculation of adsorptive capacity, q_e was done with the aid of equation 2,

$$q_e = \frac{(C_i - C_f) \times V}{M} \quad (2)$$

Where C_i, C_f, V, and M are given as the phenol initial concentration (mg L⁻¹), phenol final concentration (mg L⁻¹), volume of phenol (L) and mass of SH (g), respectively.

From the concentration study, the data obtained was analysed using Langmuir model (LM) (Langmuir, 1918) and Freundlich model (FM) (Freundlich, 1906), and their linear equations are presented in equations 3 and 4, respectively. The Langmuir model proposed a monolayer adsorption of adsorbate on the adsorbent surface, while Freundlich proposed a multilayer adsorption mechanism (Nnaji et al., 2023). The influence of adsorption time on phenol removal supplied the data which was examined by employing pseudo-first-order (PFO) (Lagergren, 1898) and pseudo-second-order (PSO) (Ho & McKay, 1999) kinetic models and whose linear equations are given in equations 5 and 6, respectively. The thermodynamic parameters were obtained from equations 7, 8, and 9 (Nnaji et al., 2023).

$$\frac{C_f}{q_e} = \frac{1}{b_L q_{max}} + \frac{C_f}{q_{max}} \quad (3)$$

$$\ln q_e = \ln K_F + \frac{1}{n_F} \ln C_f \quad (4)$$

$$\ln(q_e - q_t) = \ln q_e - k_1 t \quad (5)$$

$$\frac{t}{q_t} = \frac{1}{k_2 q_e^2} + \frac{1}{q_e} t \quad (6)$$

$$\ln K = \frac{\Delta S_{ads}}{R} - \frac{\Delta H_{ads}}{RT} \quad (7)$$

$$K = \frac{q_e}{C_f} \quad (8)$$

$$\Delta G_{ads} = \Delta H_{ads} - T \Delta S_{ads} \quad (9)$$

Where b_L is the LM constant (L mg⁻¹); q_{max} is the LM maximum adsorptive capacity (mg g⁻¹); q_e is the quantity of phenol adsorbed per unit weight of SH (mg g⁻¹); C_f is the phenol final concentration (mg L⁻¹); K_F is the FM constant (L g⁻¹); n_F is the intensity of adsorption; k₁ is the rate constant of PFO (min⁻¹); q_t is the quantity of phenol adsorbed (mg g⁻¹) at time, t (min); k₂ is the rate constant of PSO (g mg⁻¹ min⁻¹); K is equilibrium constant; R is the gas constant; ΔH_{ads} is change in enthalpy; ΔS_{ads} is change

in entropy; T is absolute temperature (K) and ΔG_{ads} is change in Gibbs free energy (Nnaji et al., 2023).

RESULTS AND DISCUSSION

Characterisation of SH

The pH_{zpc} of SH adsorbent was 6.2, as seen in Figure 1. At this pH, a positive charge equated negative charge, leaving a zero-net charge on the SH surface. Above this pH, the surface was negative; below this value, the surface was positive (de la Luz-asunción et al., 2015). The FTIR of SH adsorbent shown in Figure 2 had peaks assigned as: O-H (stretch), C=C (stretch), C=O, C-H (bend), O-H (bend), and C-O corresponding to wavenumbers of 3450, 2022, 1637, 1420, 1274 and 1024 cm^{-1} , respectively. These functional groups are essential for adsorption through several mechanisms (Xiang et al., 2020). The Sear surface area of the SH was calculated to give 77.40 $m^2 g^{-1}$.

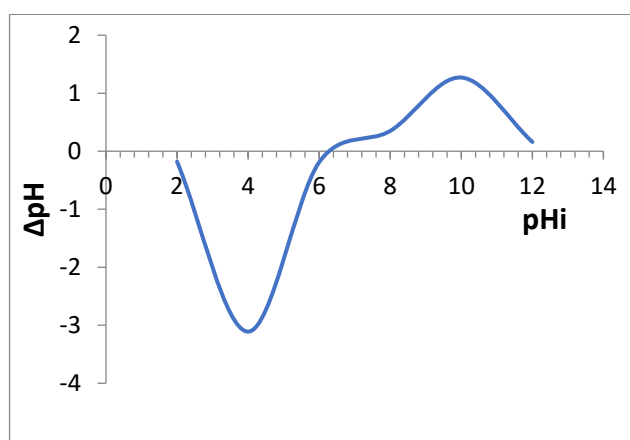


Figure 1: The pH at zero point charge of sorghum husk adsorbent

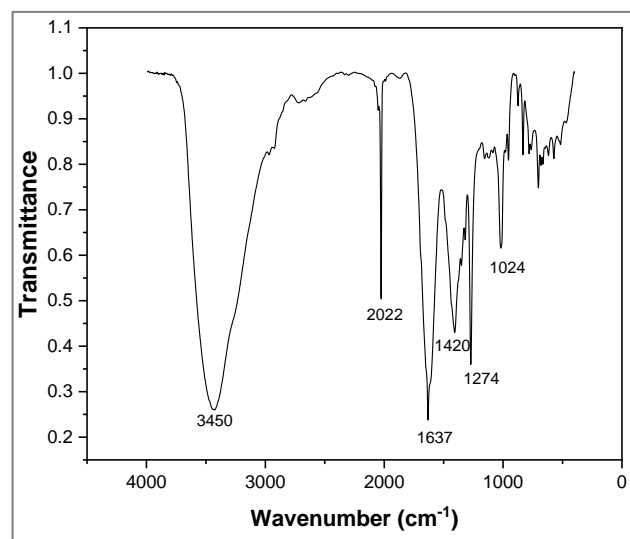


Figure 2: Sorghum husk FTIR spectrum

Influence of pH study

The adsorptive capability of SH, depicted in Figure 3, increased steadily when the pH increased from 2 to 10. Optimum pH was observed at 10, where the highest adsorptive capacity was gotten. As 9.99 is the pK_a value of phenol, this implies that it is neutral below this pH and occurs as an anion above this pH (de la Luz-asunción et

al., 2015). And since the pH_{zpc} of the SH adsorbent was 6.2, which shows that the surface of the adsorbent would be negative above this pH and given that phenol would be neutral, the mechanism of adsorption should be non-electrostatic.

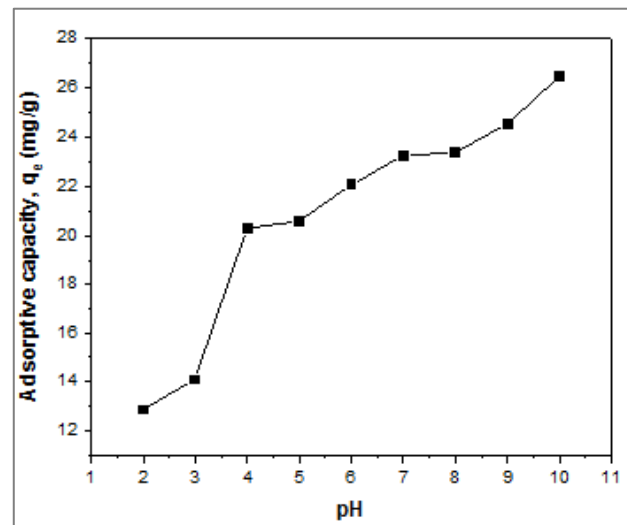


Figure 3: Influence of pH on the adsorptive capacity of sorghum husk adsorbent (initial phenol conc. = 50 mg/L, temperature = 25 °C, and adsorbent dose = 30 mg)

Influence of adsorbent dose study

As displayed in Figure 4, the adsorptive capacity of SH adsorbent was lowered as the adsorbent dose became higher. Hence, the highest adsorptive capacity was achieved with the least weight of the adsorbent used (5 mg). This trend resulted from a total coverage of the adsorbent binding sites by the phenol molecules at lower adsorbent doses. Also, at higher adsorbent doses, competition between the adsorbent particles decreases the active sites (Guo et al., 2019). Another explanation for this trend is that adsorbent particles can accumulate at higher doses, which obstructs the diffusion path for the adsorbate molecules. The same trend was observed when activated carbon obtained from *Saccharum officinarum* was employed for the uptake of phenol (Darla et al., 2023).

Adsorption equilibrium

Figure 5 depicted that the adsorptive capacity of SH adsorbent increased as the concentration of phenol was raised from 3 – 70 $mg L^{-1}$. This is ascribed to more mass transfer of phenol due to a higher force, which drives the concentration gradient (Darla et al., 2023; Nnaji et al., 2023). Researchers who used *Luffa cylindrica* fibers for the adsorption of phenol (Abdelwahab, 2014) reported a similar trend. Freundlich isotherm model (FM) gave more fitting to the adsorption data compared to the Langmuir model (LM) due to its higher correlation factor, R^2 as seen in Table 1. This implies that there was multilayer adsorption of phenol by SH adsorbent. The Langmuir maximum adsorptive capacity, q_{max} of SH was 63.69 $mg g^{-1}$ and the R_L which is a separation factor and an indicator of a favourable adsorption, was within the acceptable limit of 0 to 1 (de la Luz-asunción et al., 2015). The Freundlich constant, n_F was within 1 to 10, thereby supporting the

favourability of phenol adsorption using SH (Nnaji et al., 2023).

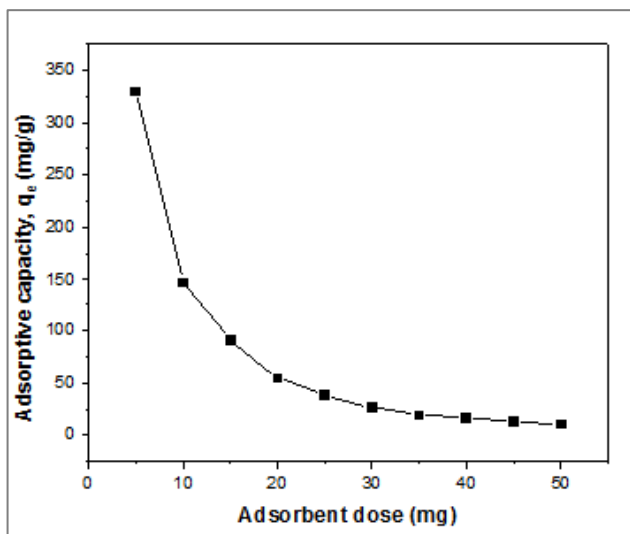


Figure 4: Influence of adsorbent dose (mg) on the adsorptive capacity of sorghum husk adsorbent (initial phenol conc. = 50 mg/L, temperature = 25 °C and pH = 10)

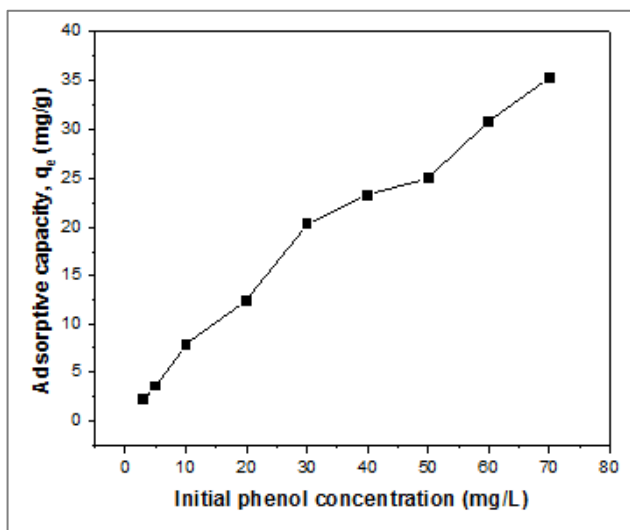


Figure 5: Influence of phenol initial concentration (mg/L) on the adsorptive capacity of sorghum husk adsorbent (adsorbent dose = 30 mg, temperature = 25 °C and pH = 10)

Table 1: Phenol adsorption isotherm parameters using SH

Adsorption isotherm model	Parameters	
LM	q_{max} (mg/g)	63.694
	b_L (L/mg)	0.022
	R_L	0.229
	R^2	0.902
FM	K_F	1.714
	n_F	1.266
	R^2	0.985

Adsorption kinetics

As seen in Figure 6, the adsorptive capacity of SH increased as the contact time moved from 0.5 to 180 min at 20, 35, and 55 °C. Initially, there was a rapid uptake of

phenol by the adsorbent as a result of adequate empty active sites on its surface. After 30 min, phenol adsorption was reduced because of the full coverage of the active sites by the phenol molecules (Kong et al., 2020). Ingole et al. (2016) reported a trend similar to this when activated carbon prepared from banana peel was utilised for the adsorptive removal of phenol. The PFO and PSO kinetic models were used to analyse the data obtained from studying the influence of contact time. As shown in Table 2, the kinetics followed PSO as its correlation factor was higher than that of the PFO model.

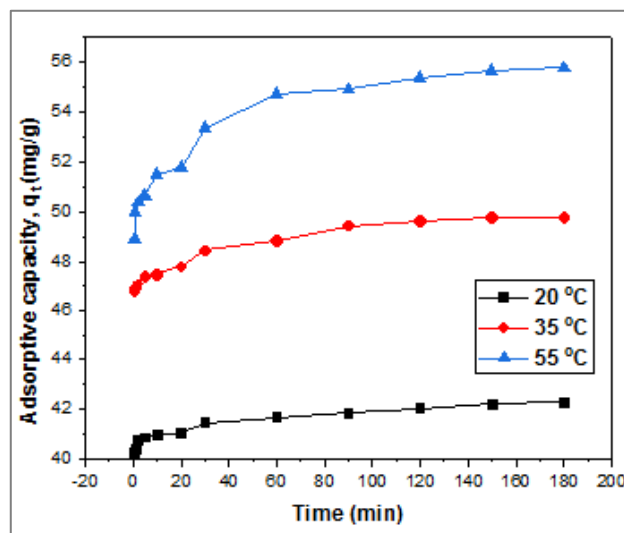


Figure 6: Influence of contact time (min) at varying temperatures on the adsorptive capacity of sorghum husk adsorbent (adsorbent dose = 30 mg, phenol concentration = 50 mg/L and pH = 10)

Table 2: Phenol adsorption kinetic parameters using SH

Adsorptive kinetic model	20 °C	35 °C	55 °C
Experimental q_e (mg g ⁻¹)	42.277	49.785	55.767
PFO			
Calculated q_e (mg g ⁻¹)	13.003	8.877	12.453
k_1 (min ⁻¹)	0.001	0.002	0.004
R^2	0.859	0.889	0.851
PSO			
Calculated q_e (mg g ⁻¹)	42.194	49.751	55.866
k_2	0.071	0.044	0.024
R^2	1.000	1.000	1.000

Adsorption thermodynamics

To determine the heat, randomness, and spontaneity of the phenol adsorption using SH adsorbent, the enthalpy, entropy, and Gibbs free energy were calculated from the slope and intercept of the graph presented in Figure 7. From evaluating the thermodynamic parameters as presented in Table 3, the adsorption process was endothermic as ΔH_{ads} was positive, random as ΔS_{ads} was positive, and spontaneous because ΔG_{ads} was negative and the level of spontaneity increased as temperature increased from 20 to 55 °C. The enthalpy value which was 12.325 kJ mol⁻¹ indicated physical adsorption (Amar et al., 2021).

Proposed mechanism of adsorption

The optimum pH for phenol adsorption by SH was 10, which was higher than the pHzpc (6.2), showing that the SH surface was negative at this pH. Phenol exists as an anion at the pH of 10, and this entails that the adsorption mechanism was mainly by non-electrostatic interactions such as hydrophobic, hydrogen, and π - π interactions. This correlates with the heat of adsorption value from thermodynamics which suggested physical adsorption as the adsorption mechanism.

Comparison of the adsorptive capacities of some adsorbents

The q_{max} of SH adsorbent was compared with those of other adsorbents that have been used for the adsorption of phenol from literature, and this is displayed in Table 4. As shown in the table, the q_{max} value of SH adsorbent was higher than most of the adsorbents used in their pristine form, while the adsorbents activated had higher q_{max} values than it.

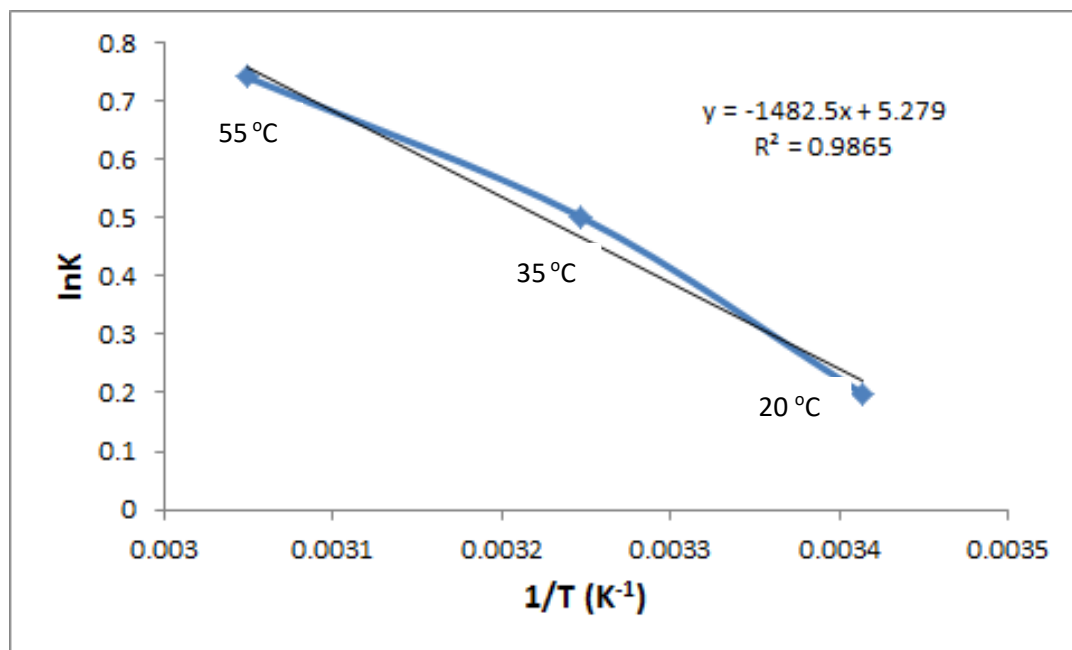


Figure 7: The plot of lnK against 1/T at 20, 35 and 55 °C

Table 3: Phenol adsorption thermodynamic parameters using SH

ΔH_{ads} (kJ mol ⁻¹)	ΔS_{ads} (J mol ⁻¹ K ⁻¹)	ΔG_{ads} (kJ mol ⁻¹)		
		20 °C	35 °C	55 °C
12.325	43.890	-0.534	-1.192	-2.070

Table 4: Comparing the Langmuir maximum adsorptive capacities (q_{max}) of some adsorbents

Adsorbents	q_{max} (mg/g)	Reference
Exfoliated graphite	2.14	(Tshemese et al., 2021)
Moroccan clay/Hematite composite	20.10	(Dehmani et al., 2023)
Rice husk activated carbon	215.27	(Lv et al., 2020)
Paper waste	7.02	(Sabbar, 2019)
<i>Luffa cylindrica</i> fibers	9.25	(Abdelwahab, 2014)
<i>Toona sinensis</i> leaves porous carbon	350.00	(Kong et al., 2020)
Banana leaves activated carbon	80.65	(Ingole et al., 2016)
Clay	83.33	(Amar et al., 2021)
Aluminium oxide nanoparticles	16.97	(Safwat et al., 2022)
Tobacco residues activated carbon	17.83	(Kilic et al., 2011)
Oily sludge activated carbon	434.00	(Mojoudi et al., 2019)
Na-bentonite	23.98	(Asnaoui et al., 2022)
Sorghum husk	63.69	This study

CONCLUSION

The adsorptive capacity of phenol using sorghum husk increased when pH, initial concentration, contact time, and temperature increased but reduced at higher adsorbent dose. The adsorption followed the FM more than LM, and the Langmuir maximum adsorptive capacity

was 63.69 mg g⁻¹. The PSO model fitted the kinetic data better, and the parameters obtained from the adsorption thermodynamics showed that the process was endothermic, random, and spontaneous. The proposed adsorption mechanism was physical adsorption. Even though the pristine sorghum husk was effective in the adsorption of phenol from water, it should be activated

using heat and chemicals, and then compare its adsorptive capacity to those of the activated adsorbents.

REFERENCES

- Abate, G. Y., Alene, A. N., Habte, A. T., & Getahun, D. M. (2020). Adsorptive removal of malachite green dye from aqueous solution onto activated carbon of *Catha edulis* stem as a low cost bio-adsorbent. *Environmental Systems Research*, 9(29). [\[Crossref\]](#)
- Abdelwahab, O. (2014). Adsorption of phenol from aqueous solutions by *Luffa cylindrica* fibers: Kinetics, isotherm and thermodynamic studies. *The Egyptian Journal of Aquatic Research*, 39(4), 215–223. [\[Crossref\]](#)
- Amar, A., Loulidi, I., Kali, A., Boukhlifi, F., Hadey, C., & Jabri, M. (2021). Physicochemical Characterization of Regional Clay: Application to Phenol Adsorption. *Applied and Environmental Soil Science*, 2021, 1–9. [\[Crossref\]](#)
- Asnaoui, H., Dehmani, Y., Khalis, M., & Hachem, E. (2022). Adsorption of phenol from aqueous solutions by Na–bentonite: kinetic, equilibrium and thermodynamic studies. *International Journal of Environmental Analytical Chemistry*, 102(13), 3043–3057. [\[Crossref\]](#)
- Darla, U. R., Lataye, D. H., Kumar, A., Pandit, B., & Ubaidullah, M. (2023). Adsorption of phenol using adsorbent derived from *Saccharum officinarum* biomass: optimization, isotherms, kinetics, and thermodynamic study. *Scientific Reports*, 1–13. [\[Crossref\]](#)
- de la Luz-asunción, M., Sánchez-Mendieta, V., Martínez-Hernández, A. I., Castaño, V. M., & Velasco-Santos, C. (2015). Adsorption of Phenol from Aqueous Solutions by Carbon Nanomaterials of One and Two Dimensions: Kinetic and Equilibrium Studies. *Journal of Nanomaterials*, 2015(1), 405036. [\[Crossref\]](#)
- Dehmani, Y., Mobarak, M., Oukhrib, R., Dahbi, A., Mohsine, A., Lamhasni, T., Tahri, Y., Ahlafi, H., Abouarnadasse, S., Lima, E. C., & Badawi, M. (2023). Adsorption of phenol by a Moroccan clay/Hematite composite: Experimental studies and statistical physical modeling. *Journal of Molecular Liquids*, 386(15), 1220508. [\[Crossref\]](#)
- Freundlich, H. (1906). Over the adsorption in solution. *Journal of Physical Chemistry*, 57, 1100–1107.
- Guo, X., He, C., Sun, X., Liang, X., Chen, X., & Liu, X. Y. (2019). Adsorption of phenol from aqueous solution by four types of modified attapulgites. *International Journal of Environmental Science and Technology*, 16, 793–800. [\[Crossref\]](#)
- Ho, Y. S., & McKay, G. (1999). Batch lead(II) removal from aqueous solution by peat: Equilibrium and kinetics. *Process Safety and Environmental Protection*, 77(3), 165–173. [\[Crossref\]](#)
- Ingole, R. S., Lataye, D. H., & Dhorabe, P. T. (2016). Adsorption of Phenol onto Banana Peels Activated Carbon. *Journal of Civil Engineering*, 00, 1–11. [\[Crossref\]](#)
- Issabayeva, G., Hang, S. Y., Wong, M. C., & Aroua, M. K. (2018). A review on the adsorption of phenols from wastewater onto diverse groups of adsorbents. *Reviews in Chemical Engineering*, 34(6), 855–873. [\[Crossref\]](#)
- Kilic, M., Apaydin-varol, E., & Pütün, A. E. (2011). Adsorptive removal of phenol from aqueous solutions on activated carbon prepared from tobacco residues: Equilibrium, kinetics and thermodynamics. *Journal of Hazardous Materials Journal*, 189, 397–403. [\[Crossref\]](#)
- Kong, X., Gao, H., Song, X., Deng, Y., & Zhang, Y. (2020). Adsorption of phenol on porous carbon from *Toona sinensis* leaves and its mechanism. *Chemical Physics Letters*, 739, 137046. [\[Crossref\]](#)
- Lagergren, S. K. (1898). About the theory of so-called adsorption of soluble substances. *Sven. Vetenskapsakad. Handlingar*, 24, 1–39.
- Langmuir, I. (1918). The adsorption of gases on plane surfaces of glass, mica and platinum. *Journal of the American Chemical Society*, 40, 1361–1403. [\[Crossref\]](#)
- Lv, S., Li, C., Mi, J., & Meng, H. (2020). A functional activated carbon for efficient adsorption of phenol derived from pyrolysis of rice husk , KOH-activation and EDTA-4Na-modification. *Applied Surface Science*, 510(November 2019), 145425. [\[Crossref\]](#)
- Mojoudi, N., Mirghaffari, N., Soleimani, M., Shariatmadari, H., Belver, C., & Bedia, J. (2019). Phenol adsorption on high microporous activated carbons prepared from oily sludge: equilibrium, kinetic and thermodynamic studies. *Scientific Reports*, 9, 1–12. [\[Crossref\]](#)
- Nnaji, N. J. N., Sonde, C. U., Nwanji, O. L., Ezech, G. C., Onuigbo, A. U., Ojukwu, A. M., Mbah, P. C., Omowumi, A., Unoka, E. C., Otedo, J. O., & Onuegbu, T. U. (2023). *Dacryodes edulis* leaf derived biochar for methylene blue biosorption. *Journal of Environmental Chemical Engineering*, 11(3), 109638. [\[Crossref\]](#)
- Sabbar, H. A. (2019). Adsorption of Phenol from Aqueous Solution using Paper Waste. *Iraqi Journal of Chemical and Petroleum Engineering*, 20(1), 23–29. [\[Crossref\]](#)
- Safwat, S. M., Mohamed, N. Y., Meshref, M. N. A., & Elawwad, A. (2022). Adsorption of Phenol onto Aluminum Oxide Nanoparticles: Performance Evaluation, Mechanism Exploration, and Principal Component Analysis (PCA) of Thermodynamics. *Adsorption Science & Technology*, 2022, 1924117. [\[Crossref\]](#)
- Sears, G. W. (1956). Determination of Specific Surface Area of Colloidal Silica by Titration With Sodium Hydroxide. *Analytical Chemistry*, 28(12), 1981–1983. [\[Crossref\]](#)
- Sellaoui, L., Kehili, M., Lima, E. C., Thue, P. S., Bonilla-petriciolet, A., Lamine, A. Ben, Dotto, G. L., & Erto, A. (2019). Adsorption of phenol on microwave-assisted activated carbons: Modelling and interpretation. *Journal of Molecular Liquids*, 274, 309–314. [\[Crossref\]](#)
- Shaikhiev, I. G. (2024). Using Sorghum Waste and Biomass Components to Remove Pollutants from Aquatic Environments (a Literature Review).

- Materials International*, 6(4), 1–20. [\[Crossref\]](#)
- Tatah, V. S., Otitoju, O., Ezeonu, C. S., Onwurah, I. N. E., & C, I. K. L. (2017). Characterization and Adsorption Isotherm Studies of Cd (II) And Pb (II) Ions Bioremediation from Aqueous Solution Using Unmodified Sorghum Husk. *Journal of Applied Biotechnology and Bioengineering*, 2(3), 1–9. [\[Crossref\]](#)
- Tshemese, S. J., Mhike, W., & Tichapondwa, S. M. (2021). Adsorption of phenol and chromium (VI) from aqueous solution using exfoliated graphite: Equilibrium, kinetics and thermodynamic studies. *Arabian Journal of Chemistry*, 14(6), 103160. [\[Crossref\]](#)
- Wang, X., Chen, A., Chen, B., & Wang, L. (2020). Adsorption of phenol and bisphenol A on river sediments: Effects of particle size, humic acid, pH and temperature. *Ecotoxicology and Environmental Safety*, 204(April), 111093. [\[Crossref\]](#)
- Xiang, W., Wan, Y., Zhang, X., Tan, Z., Xia, T., Zheng, Y., & Gao, B. (2020). Adsorption of tetracycline hydrochloride onto ball-milled biochar: Governing factors and mechanisms. *Chemosphere*, 255, 127057. [\[Crossref\]](#)
- Xu, H., Wang, B., Zhao, R., Wang, X., Pan, C., & Jiang, Y. (2022). Adsorption behavior and performance of ammonium onto sorghum straw biochar from water. *Scientific Reports*, 12, 1–11. [\[Crossref\]](#)